Polarizable molecular dynamics simulations on the conductivity of 1-methylimidazolium acetate systems: Electronic Supporting Information

Florian Joerg[a,b] and Christian Schröder*[a]

May 13, 2022

Contents

1 Force field parameters **2**
1.1 Electrostatic parameters . . . 2
1.2 Intramolecular parameters . . . 4
1.3 Lennard-Jones parameter . . . 8

2 Physico-chemical properties **9**
2.1 Conductivity and diffusion coefficients . . . 9
2.2 Haven ratio of the Nernst-Einstein relation . . . 10
2.3 Bahe-Varela fits . . . 11
2.4 Computational dielectric spectrum . . . 12
2.5 The Voronoi shell-resolved PMF . . . 13
2.6 Hydrogen bond lifetimes . . . 15

[a] *University of Vienna, Faculty of Chemistry, Department of Computational Biological Chemistry, Währingerstr. 17, A-1090 Vienna, Austria; Tel: +43 1 4277 52711; E-mail: christian.schroeder@univie.ac.at*
[b] *University of Vienna, Vienna Doctoral School in Chemistry (DoSChem), Währingerstr. 42, A-1090 Vienna, Austria*

1 Force field parameters

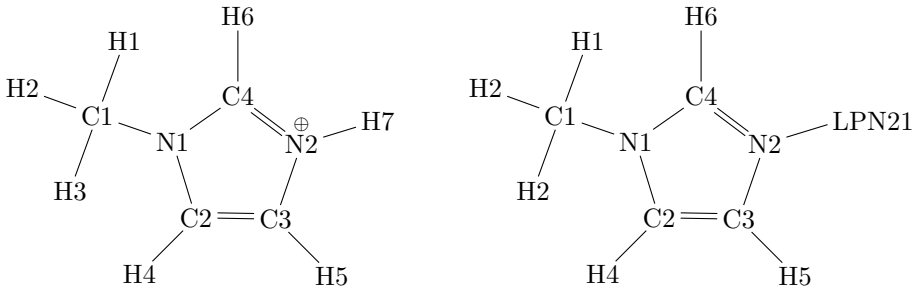

Topology of Im_1H^+ Topology of Im_1

Figure S1: Topology of Im_1H^+ and Im_1, displaying each particle with its atom name used by `CHARMM`

Figure S1 displays the topology of 1-methylimidazolium (Im_1H^+) and 1-methylimidazole (Im_1), with the name of each atom used during the MD simulation. The corresponding atom type to each atom name can be found in Table S1.

1.1 Electrostatic parameters

Partial charges (q), polarizabilities (α) and Thole parameters can also be seen for all four molecules. As no Drude particle is assigned to hydrogens, they have neither a polarizability nor a Thole value. Their corresponding polarizability was added to the parent C or N atom. Partial charges, polarizabilities and Thole parameters were not fitted during the force-matching procedure, but additional fitting using the CHELPG method was done. In the case of the the nitrogen atom of Im_1 (N2), the whole charge is carried by the lonepair (LPN21).

To increase the stability of polarizable MD simulations using Drude oscillators, usually a maximum distance of the mobile Drude particle to its polarizable atom is defined. A standard maximum distance is 0.2 Å. As shown in Fig. S2 this distance is rarely realized in our simulations and indicate stable conditions.

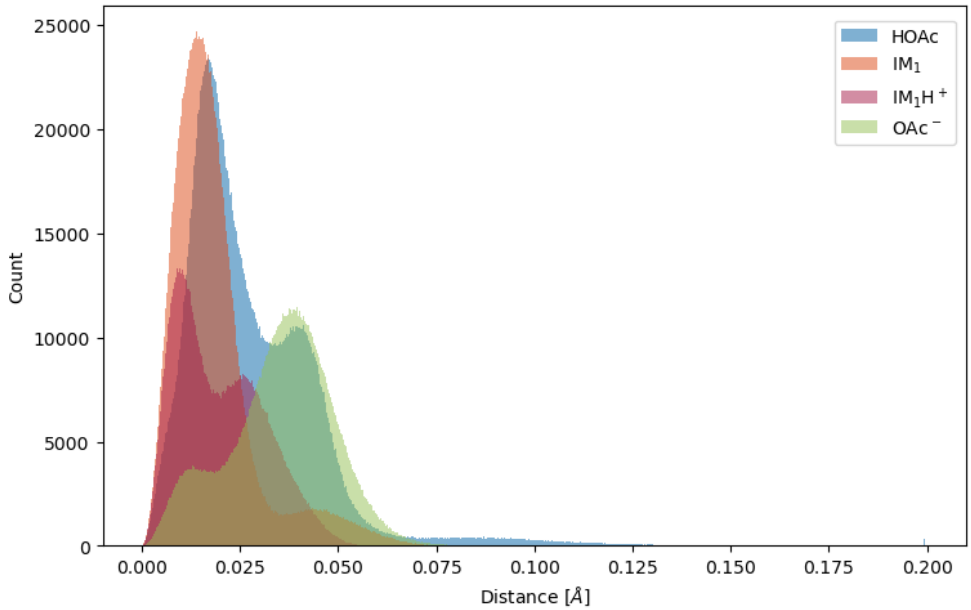

Figure S2: Histogram of the distances of the mobile Drude particles from their polarizable atoms. As clearly visible, the hard wall of 0.2 Å is rarely visited.

Table S1: Partial charges, polarizabilities and Thole parameters of the atoms for the molecules Im_1H^+ and Im_1, acetate (OAc^-), acetic acid (HOAc)

		Im_1H^+					Im_1		
atom	type	q [e]	α [Å^3]	Thole [Å]	atom	type	q [e]	α [Å^3]	Thole [Å]
C1	CD33F	−0.182	−1.181	1.1	C1	CD33G	−0.161	−1.081	1.0
H1	HDA3A	0.135			H1	HDA3A	0.094		
H2	HDA3A	0.135			H2	HDA3A	0.094		
H3	HDA3A	0.135			H3	HDA3A	0.094		
N1	ND2R5C	0.158	−0.803	1.0	N1	ND2R5A	0.140	−1.063	1.3
C2	CD2R5D	−0.107	−1.083	1.1	C2	CD2R5A	−0.369	−1.378	1.3
H4	HDR5D	0.195			H4	HDR5A	0.150		
C3	CD2R5D	−0.047	−1.083	1.1	C3	CD2R5A	0.188	−1.378	1.3
H5	HDR5D	0.192			H5	HDR5A	0.053		
C4	CD2R5E	−0.023	−1.253	1.2	C4	CD2R5B	0.118	−0.868	1.3
H6	HDR5E	0.203			H6	HDR5B	0.073		
N2	ND2R5C	−0.157	−0.803	1.0	N2	ND2R5B	0.000	−0.840	1.0
H7	HDP1A	0.363			LPN21	LPD	−0.474		

		OAc^-					HOAc		
atom	type	q [e]	α [Å^3]	Thole [Å]	atom	type	q [e]	α [Å^3]	Thole [Å]
C1	CD2O2A	0.708	−1.016	0.899	C1	CD2O3A	0.858	−1.207	0.708
C2	CD33A	−0.194	−1.681	1.414	C2	CD33C	−0.300	−2.114	0.750
H1	HDA3A	0.004			H1	HDA3A	0.092		
H2	HDA3A	0.004			H2	HDA3A	0.092		
H3	HDA3A	0.004			H3	HDA3A	0.092		
O1	OD2C2A	0.003	−0.699	2.399	O1	OD2C3A	0.000	−0.922	1.539
O2	OD2C2A	0.003	−0.699	2.399	O2	OD31F	0.000	−1.280	1.124
					H	HDP1A	0.374		
LPO11	LPD	−0.383			LPO11	LPD	−0.319		
LPO12	LPD	−0.383			LPO12	LPD	−0.319		
LPO21	LPD	−0.383			LPO21	LPD	−0.285		
LPO22	LPD	−0.383			LPO22	LPD	−0.285		

1.2 Intramolecular parameters

Table S2: Bonded parameters used in this study. Drude - parent atom force constants are uniformly set to $1000\,\mathrm{kcal\,mol^{-1}\,\AA^{-2}}$.

Atoms	k_b [$\mathrm{kcal\,mol^{-1}\,\AA^{-2}}$]	b_0 [Å]
CD2R5A - HDR5A	365.0	1.083
CD2R5A - CD2R5A	516.3	1.468
CD2R5B - HDR5B	340.0	1.090
CD2R5D - HDR5D	365.0	1.083
CD2R5D - CD2R5D	548.0	1.435
CD2R5E - HDR5E	340.0	1.090
CD33F - HDA3A	322.0	1.111
CD33G - HDA3A	322.0	1.111
CD33A - CD2O2A	110.0	1.535
CD33A - HDA3A	322.0	1.111
CD33C - HDA3A	322.0	1.111
CD33C - CD2O3A	133.0	1.510
ND2R5A - CD2R5A	413.4	1.422
ND2R5A - CD2R5B	430.1	1.429
ND2R5A - CD33G	215.8	1.424
ND2R5B - CD2R5A	328.0	1.416
ND2R5B - CD2R5B	486.5	1.368
ND2R5C - HDP1A	466.0	1.000
ND2R5C - CD2R5D	394.5	1.405
ND2R5C - CD2R5E	500.4	1.378
ND2R5C - CD33F	260.1	1.469
OD2C2A - CD2O2A	527.0	1.250
OD2C3A - CD2O3A	730.0	1.200
OD31F - HDP1A	480.4	0.969
OD31F - CD2O3A	205.5	1.269
LPD - ND2R5B	0.0	0.000
LPD - OD2C2A	0.0	0.000
LPD - OD2C3A	0.0	0.000
LPD - OD31F	0.0	0.000

Table S3: Angle parameters used in this study

Atoms	k_θ [kcal mol^{-1} rad^{-2}]	θ_0 [°]	k_θ UB [kcal mol^{-1} rad^{-2}]	θ_0 UB [°]
HDA3A - CD33F - HDA3A	35.50	108.4000	5.4000	1.8020
HDA3A - CD33G - HDA3A	35.50	108.4000	5.4000	1.8020
HDA3A - CD33A - HDA3A	35.50	108.4000	5.4000	1.8020
HDA3A - CD33C - HDA3A	35.50	108.4000	5.4000	1.8020
CD2O2A - CD33A - HDA3A	27.70	107.5000	25.3000	2.1670
CD2O3A - OD31F - HDP1A	58.90	110.2000	15.1000	2.3770
CD2O3A - CD33C - HDA3A	33.00	109.5000	30.0000	2.1630
CD2R5A - CD2R5A - HDR5A	36.42	147.9600	11.3300	0.0000
CD2R5B - ND2R5A - CD2R5A	79.78	82.9800	0.0000	0.0000
CD2R5B - ND2R5B - CD2R5A	94.37	83.7800	0.0000	0.0000
CD2R5D - ND2R5C - HDP1A	28.72	112.7000	10.7900	2.2746
CD2R5D - CD2R5D - HDR5D	36.73	146.2500	9.4500	0.0000
CD2R5E - ND2R5C - HDP1A	27.82	105.6100	16.7400	2.5139
CD2R5E - ND2R5C - CD2R5D	94.00	87.9000	0.0000	0.0000
CD33A - ND2R5A - CD2R5A	45.91	118.9500	0.0000	0.0000
CD33A - ND2R5A - CD2R5B	42.22	117.9900	0.0000	0.0000
CD33A - ND2R5C - CD2R5D	49.24	123.2400	0.0000	0.0000
CD33A - ND2R5C - CD2R5E	49.11	123.0200	0.0000	0.0000
ND2R5A - CD33A - HDA3A	51.72	107.4500	0.0000	0.0000
ND2R5A - CD2R5A - HDR5A	40.89	133.5300	12.1400	0.5612
ND2R5A - CD2R5B - HDR5B	45.01	144.5300	14.3200	0.0000
ND2R5A - CD2R5A - CD2R5A	88.69	84.8200	0.0000	0.0000
ND2R5B - CD2R5A - HDR5A	45.44	136.2200	9.9800	0.0396
ND2R5B - CD2R5B - HDR5B	44.18	144.5300	14.1600	0.2283
ND2R5B - CD2R5A - CD2R5A	96.13	90.7700	0.0000	0.0000
ND2R5B - CD2R5B - ND2R5A	101.77	95.9400	0.0000	0.0000
ND2R5C - CD33A - HDA3A	56.76	107.5500	0.0000	0.0000
ND2R5C - CD2R5D - HDR5D	43.35	133.1900	8.3300	0.0000
ND2R5C - CD2R5E - HDR5E	39.84	137.7700	8.5600	0.0000
ND2R5C - CD2R5D - CD2R5D	97.52	85.8900	0.0000	0.0000
ND2R5C - CD2R5E - ND2R5C	111.97	97.2300	0.0000	0.0000
OD2C2A - CD2O2A - CD33A	23.80	123.0000	34.9000	2.3910
OD2C2A - CD2O2A - OD2C2A	83.70	127.9000	128.8000	2.3790
OD2C3A - CD2O3A - CD33C	70.00	126.0000	20.0000	2.4420
OD31F - CD2O3A - CD33C	48.50	113.4000	26.8000	2.3370
OD31F - CD2O3A - OD2C3A	98.80	117.5000	178.3000	2.4240

Table S4: Dihedral parameters used in this study

Atoms	k_ϕ [kcal mol^{-1}]	Multiplicity	δ [°]
HDR5A - CD2R5A - CD2R5A - HDR5A	0.87	2	180.0000
HDR5D - CD2R5D - CD2R5D - HDR5D	1.14	2	180.0000
CD2R5A - ND2R5A - CD33G - HDA3A	0.20	3	0.0000
CD2R5A - ND2R5A - CD2R5B - HDR5B	3.41	2	180.0000
CD2R5A - ND2R5B - CD2R5B - HDR5B	5.44	2	180.0000
CD2R5B - ND2R5A - CD33G - HDA3A	0.16	3	0.0000
CD2R5B - ND2R5A - CD2R5A - HDR5A	3.52	2	180.0000
CD2R5B - ND2R5B - CD2R5A - HDR5A	5.22	2	180.0000
CD2R5B - ND2R5A - CD2R5A - CD2R5A	16.78	2	180.0000
CD2R5B - ND2R5B - CD2R5A - CD2R5A	15.37	2	180.0000
CD2R5D - ND2R5C - CD33F - HDA3A	0.19	3	0.0000
CD2R5D - ND2R5C - CD2R5E - HDR5E	3.58	2	180.0000
CD2R5E - ND2R5C - CD33F - HDA3A	0.08	3	0.0000
CD2R5E - ND2R5C - CD2R5D - HDR5D	3.96	2	180.0000
CD2R5E - ND2R5C - CD2R5D - CD2R5D	14.88	2	180.0000
CD33G - ND2R5A - CD2R5A - HDR5A	0.41	2	180.0000
CD33G - ND2R5A - CD2R5B - HDR5B	0.39	2	180.0000
CD33F - ND2R5C - CD2R5D - HDR5D	0.81	2	180.0000
CD33F - ND2R5C - CD2R5E - HDR5E	1.32	2	180.0000
CD33G - ND2R5A - CD2R5A - CD2R5A	2.89	2	180.0000
CD33F - ND2R5C - CD2R5D - CD2R5D	3.17	2	180.0000
ND2R5A - CD2R5A - CD2R5A - HDR5A	3.93	2	180.0000
ND2R5B - CD2R5A - CD2R5A - HDR5A	3.85	2	180.0000
ND2R5B - CD2R5A - CD2R5A - ND2R5A	20.41	2	180.0000
ND2R5C - CD2R5D - CD2R5D - HDR5D	4.43	2	180.0000
ND2R5C - CD2R5D - CD2R5D - ND2R5C	22.94	2	180.0000
HDP1A - ND2R5C - CD2R5D - HDR5D	0.78	2	180.0000
HDP1A - ND2R5C - CD2R5E - HDR5E	1.17	2	180.0000
HDP1A - ND2R5C - CD2R5D - CD2R5D	3.78	2	180.0000
HDP1A - OD31F - CD2O3A - CD33C	3.76	2	180.0000
CD2R5A - ND2R5B - CD2R5B - ND2R5A	19.75	2	180.0000
CD2R5A - ND2R5A - CD2R5B - ND2R5B	16.21	2	180.0000
CD33G - ND2R5A - CD2R5B - ND2R5B	4.20	2	180.0000
HDP1A - ND2R5C - CD2R5E - ND2R5C	4.65	2	180.0000
CD2R5D - ND2R5C - CD2R5E - ND2R5C	18.25	2	180.0000
CD33F - ND2R5C - CD2R5E - ND2R5C	6.55	2	180.0000
HDA3A - CD33A - CD2O2A - OD2C2A	0.42	3	180.0000
HDP1A - OD31F - CD2O3A - OD2C3A	1.11	2	180.0000
HDA3A - CD33C - CD2O3A - OD2C3A	0.00	3	180.0000
HDA3A - CD33C - CD2O3A - OD31F	0.00	6	180.0000

Table S5: Improper parameters used in this study

Atoms	k_ϕ [kcal mol^{-1} rad^{-2}]	δ [°]
ND2R5A - CD2R5B - CD2R5A - CD33G	0.45	0.0000
ND2R5C - CD2R5E - CD2R5D - HDP1A	0.45	0.0000
ND2R5C - CD2R5E - CD2R5D - CD33F	0.45	0.0000
CD2R5E - ND2R5C - ND2R5C - HDR5E	0.50	0.0000
CD2R5A - CD2R5A - ND2R5A - HDR5A	0.50	0.0000
CD2R5A - CD2R5A - ND2R5B - HDR5A	0.50	0.0000
CD2R5B - ND2R5A - ND2R5B - HDR5B	0.50	0.0000
CD2R5D - CD2R5D - ND2R5C - HDR5D	0.50	0.0000
OD2C2A - CD33A - OD2C2A - CD2O2A	71.00	0.0000
OD2C3A - CD33C - OD31F - CD2O3A	85.00	0.0000

1.3 Lennard-Jones parameter

Adding Drude particles to a non-polarizable force field results in a double-counting of dispersion interactions. The Lennard-Jones parameters in the non-polarizable force field take already the average effect of these interactions into account.

Instead of reparametrizing all Lennard-Jones interactions after switching on the Drude oscillators, we scale the ϵ-values according to the empirical equation

$$\epsilon_\beta^{LJ} = \epsilon_\beta^{LJ,unscaled} \frac{\Big(max(\alpha_\beta) - \alpha_\beta\Big) + \lambda\, max(\alpha_\beta)}{max(\alpha_\beta) + \lambda \Big(max(\alpha_\beta) - \alpha_\beta\Big)} \tag{1}$$

$\max(\alpha_\beta)$ is the largest atomic polarizability in our system, *i.e.* the polarizability of the atom type CD33C of HOAc. The Lennard-Jones σ is untouched by this scaling.

In the CHARMM force field, the distance for the minimum of the Lennard-Jones potential is used. It can be easily calculated from the Lennard-Jones σ:

$$r_{min} = 2^{1/6} \cdot \sigma \tag{2}$$

$$r_{min}/2 = 2^{-5/6} \cdot \sigma \tag{3}$$

Table S6: Nonbonded parameters for all heavy atoms in Im_1H^+, Im_1, OAc^-, HOAc for the scaling factors 0.25 and 0.4. Hydrogens are unaffected by the scaling and therefore not shown.

Molecule	Atoms	$\varepsilon_{\lambda=0.25}$ [kcal mol^{-1}]	$\varepsilon_{\lambda=0.4}$ [kcal mol^{-1}]	$r_{min}/2$ [Å]
Im_1H^+	CD33F	−0.0486	−0.0558	3.040
	CD2R5D	−0.0329	−0.0371	1.800
	CD2R5E	−0.0597	−0.0694	1.850
	ND2R5C	−0.0791	−0.0858	1.850
Im_1	CD33G	−0.0513	−0.0580	2.040
	CD2R5A	−0.0523	−0.0624	2.070
	CD2R5B	−0.0680	−0.0745	1.980
	ND2R5A	−0.0578	−0.0651	1.861
	ND2R5B	−0.0511	−0.0557	1.956
OAc^-	CD2O2A	−0.1566	−0.1751	1.800
	CD33A	−0.0337	−0.0436	2.040
	OD2C2A	−0.1575	−0.1687	1.910
HOAc	CD2O3A	−0.0564	−0.0651	1.650
	CD33C	−0.0195	−0.0312	1.940
	OD2C3A	−0.1141	−0.1258	1.880
	OD31F	−0.1009	−0.1180	1.710

2 Physico-chemical properties

2.1 Conductivity and diffusion coefficients

Table S7: Average boxlength L, density ρ and conductivity $\sigma(0)$ of the different systems. These values are averaged over the trajectories of the three replica.

	λ=0.25			λ=0.4		
ϕ_{IL}	L [Å]	ρ [g cm^{-3}]	$\sigma(0)$ [mS cm^{-1}]	L [Å]	ρ [g cm^{-3}]	$\sigma(0)$ [mS cm^{-1}]
0.0	49.71	0.96	-	49.25	0.99	-
0.1	49.23	0.99	1.87	48.90	1.01	1.84
0.2	48.90	1.01	2.76	48.58	1.03	2.20
0.3	48.59	1.03	2.85	48.29	1.05	2.38
0.4	48.24	1.05	2.77	48.03	1.07	1.80
0.5	47.98	1.07	1.82	47.78	1.08	1.22
0.7	47.46	1.10	0.58	47.31	1.11	0.28
0.9	47.04	1.13	0.14	46.95	1.14	0.09
1.0	46.85	1.15	0.10	46.75	1.16	0.07

Table S8: Diffusion coefficients for all four species, average of three replica

	λ=0.25				λ=0.4			
ϕ_{IL}	Im_1H^+	OAc^-	Im_1	HOAc	Im_1H^+	OAc^-	Im_1	HOAc
	$[10^{-8}$ cm^2 s$^{-1}]$				$[10^{-8}$ cm^2 s$^{-1}]$			
0.0	-	-	791.858	682.270	-	-	553.391	501.306
0.1	200.009	195.309	519.620	394.798	146.988	136.843	386.904	310.026
0.2	112.268	108.854	350.007	234.159	82.6900	80.3211	250.054	183.570
0.3	63.6601	59.6877	223.418	135.755	45.6798	44.3336	151.728	103.475
0.4	32.6145	31.0725	119.935	69.5578	23.6877	22.5152	81.5990	52.7524
0.5	15.1213	13.8313	63.0723	34.1194	10.3093	9.81508	43.3023	25.9586
0.7	2.59998	2.31557	11.0175	7.08491	1.37953	1.22568	5.87537	3.83983
0.9	0.45291	0.38553	1.55147	1.15477	0.32470	0.27562	0.87525	0.72008
1.0	0.26304	0.21010	-	-	0.17975	0.15183	-	-

2.2 Haven ratio of the Nernst-Einstein relation

Based on the diffusion coefficients, the Nernst-Einstein conductivity can be obtained via

$$\sigma_{NE} = \frac{1}{k_B\, T} \sum_k |q_k|^2\, \rho_k\, D_k \tag{4}$$

It usually overestimates the conductivity of the system as correlations between the species are ignored. This overestimation is usually quantified by the Haven ratio $(1 - \Delta)$

$$\sigma(0) = \sigma_{NE} \cdot (1 - \Delta) \tag{5}$$

However, as shown in Fig. S3 this ratio is a function of the fraction ϕ_{IL} of charged molecules and far from being constant. The Δ-parameter of the Haven ratio decreases with increasing ϕ_{IL}. In other words, the collective effects are stronger at lower content of the ions.

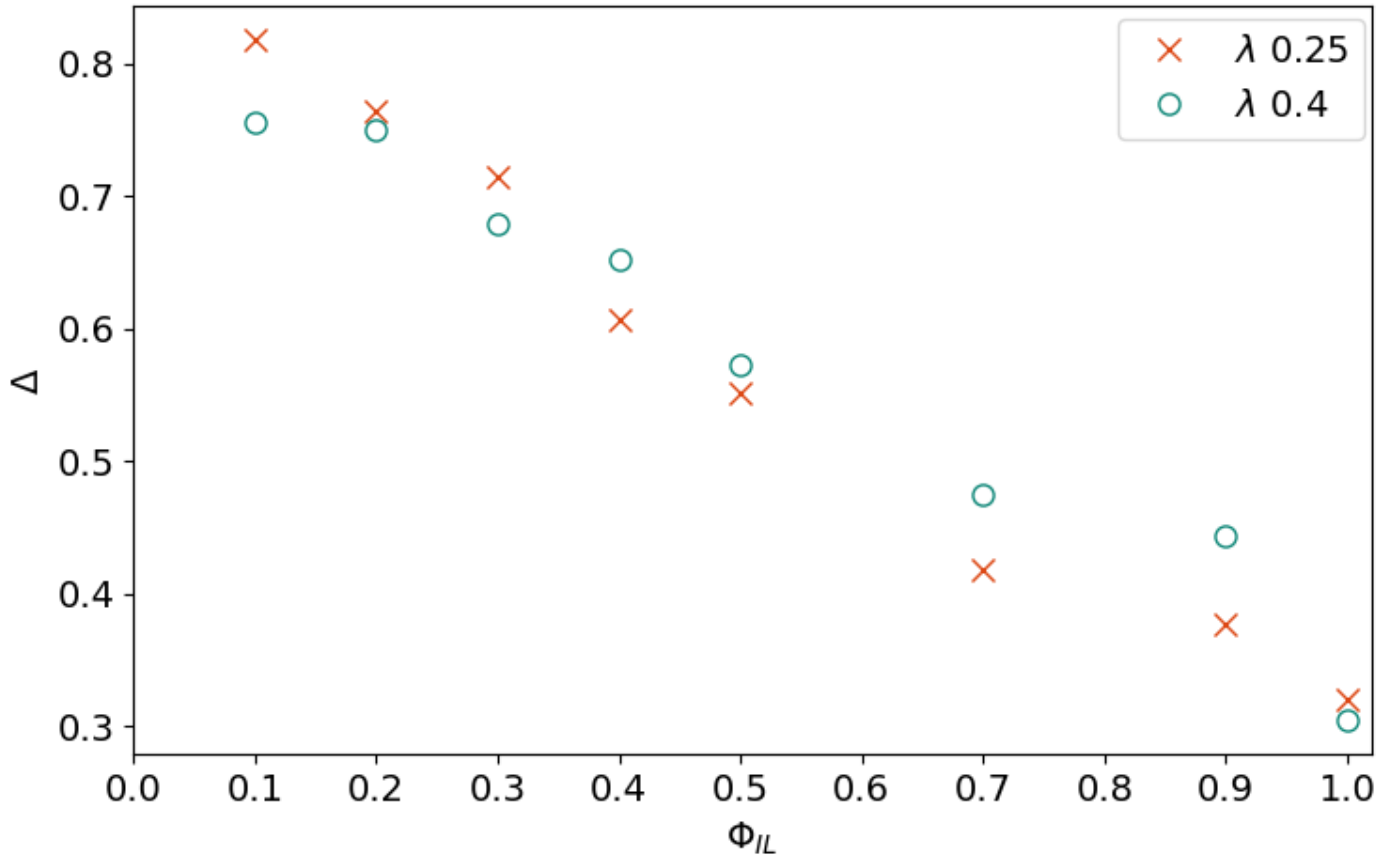

Figure S3: $\Delta(\phi_{IL})$ for λ 0.25 and 0.4.

2.3 Bahe-Varela fits

Figure S4 shows the conductivity at $\lambda = 0.25$ for the fits described in Ref. 1 also including a quadratic and cubic term. Including these terms leads to unpyhsical behaviour for $\phi_{IL} > 0.8$.

$$\frac{\sigma(0)}{max\Big(\sigma(0)\Big)} = 2\xi_{IL}(1-\xi_{IL}) \tag{6}$$

$$\frac{\sigma(0)}{max\Big(\sigma(0)\Big)} = 2\xi_{IL}(1-\xi_{IL}) + A\,\xi_{IL}(1-\xi_{IL})^2 \tag{7}$$

$$\frac{\sigma(0)}{max\Big(\sigma(0)\Big)} = 2\xi_{IL}(1-\xi_{IL}) + A\,\xi_{IL}(1-\xi_{IL})^2 + B\,\xi_{IL}(1-\xi_{IL})^3 \tag{8}$$

with $\xi_{IL} = \phi_{IL}/\phi_{IL}(max(\sigma(0)))$.

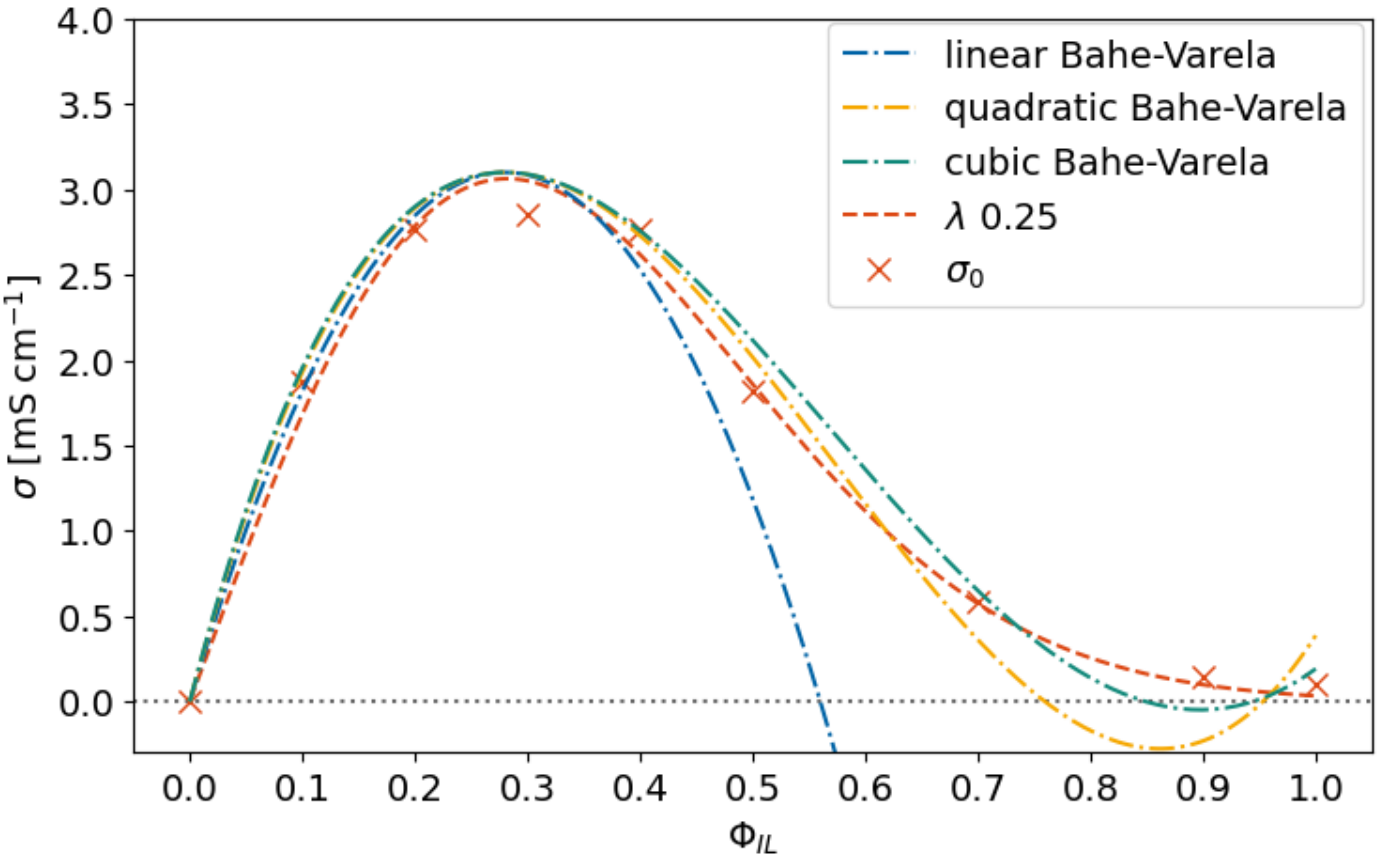

Figure S4: Fits of the conductivity at $\lambda = 0.25$ with a linear, quadratic and cubic Bahe-Varela fitfunction (Eq. 6-8).

2.4 Computational dielectric spectrum

In order to compute the high-frequency limit ϵ_∞ of our mixtures, the molecular polarizabilities α_κ and volumes V_κ of each species are needed. The dipole moments and polarizabilities are obtained from Gaussian frequency calculations on a B3LYP/6-311+G** level of theory. All dipole moments are computed with respect to the center-of-mass. The molecular volumes are estimated on statistical averages taken from Ref. 2.

Table S9: Molecular dipole moments, polarizability and volume of all species k.

Species	μ_k [D]	α_k [Å^3]	V_k [Å^3]
Im_1	4.3	8.7	125.8
HOAc	1.7	4.8	73.3
Im_1H^+	1.4	7.7	131.7
OAc^-	3.9	6.4	67.4

The high-frequency limit ϵ_∞ of the static generalized dielectric constant $\Sigma_0(0)$ can be estimated on the basis of a Clausius-Mossotti equation

$$\frac{\epsilon_\infty - 1}{\epsilon_\infty + 2} = \frac{4\pi}{3} \frac{\sum_k \phi_k \cdot \alpha_k}{\sum_k \phi_k \cdot V_k} \tag{9}$$

using an averaged molecular polarizability and and volume. These averages are weighted by the mole fraction ϕ_k of the species. Except for $\phi = 1$ (only ionic species), the high-frequency limit ϵ_∞ yields 2.2 which corresponds to a refractive index of 1.48. In case of ϕ=1.0, ϵ_∞ is 2.3. In other words, the high-frequency limit ϵ_∞ does not change as a function of the composition of our systems.

Table S10: Decomposition of the static generalized dielectric constant into contributions from each species from polarizable MD simulations applying λ=0.25 and λ=0.4.

			$\lambda = 0.4$				$\lambda = 0.25$			
ϕ_{IL}	k	c_k [mol/l]	$\epsilon(0)$	$\vartheta_0(0)$	ϵ_∞	$\Sigma_0(0)$	$\epsilon(0)$	$\vartheta_0(0)$	ϵ_∞	$\Sigma_0(0)$
0.0	Im_1	6.8	12.8	-	2.2	17.9	12.2	-	2.2	16.7
	HOAc		2.9	-			2.3	-		
0.2	Im_1H^+	1.4	0.9	11.4	2.2	33.2	1.2	12.5	2.2	36.7
	OAc^-		2.6				3.0			
	Im_1	5.7	10.5	-			11.5	-		
	HOAc		5.6	-			6.3	-		
0.3	Im_1H^+	2.2	1.6	7.9	2.2	29.8	1.3	12.1	2.2	31.3
	OAc^-		3.7				3.1			
	Im_1	5.1	9.9	-			8.2	-		
	HOAc		4.5	-			4.4	-		
1.0	Im_1H^+	8.1	1.2	2.6	2.3	9.7	0.8	2.8	2.3	10.6
	OAc^-		3.6				4.7			

The Lennard-Jones scaling parameter λ has a small influence on the static dielectric parameters. However, decreasing λ=0.40 to λ=0.25 may increase or decrease the partial permittivities $\epsilon_k(0)$. The static dielectric conductivity $\vartheta_0(0)$ seems to increase with decreasing λ in a non-uniform way.

The Cavell equation[3] reads:

$$S_k = \epsilon_k(0) = \frac{\epsilon_R}{2\epsilon_R + 1} \cdot \frac{N_A c_k}{k_B T \epsilon_0} \mu^2_{\text{eff},k} \tag{10}$$

As our simulation contains charged species, the static dielectric constant ϵ_R is the static value of the generalized dielectric constant $\Sigma_0(0)$. Using the values of Table S9 and Table S10, S_k can be correlated with $\epsilon_k(0)$ as shown in Fig. S5. The dashed

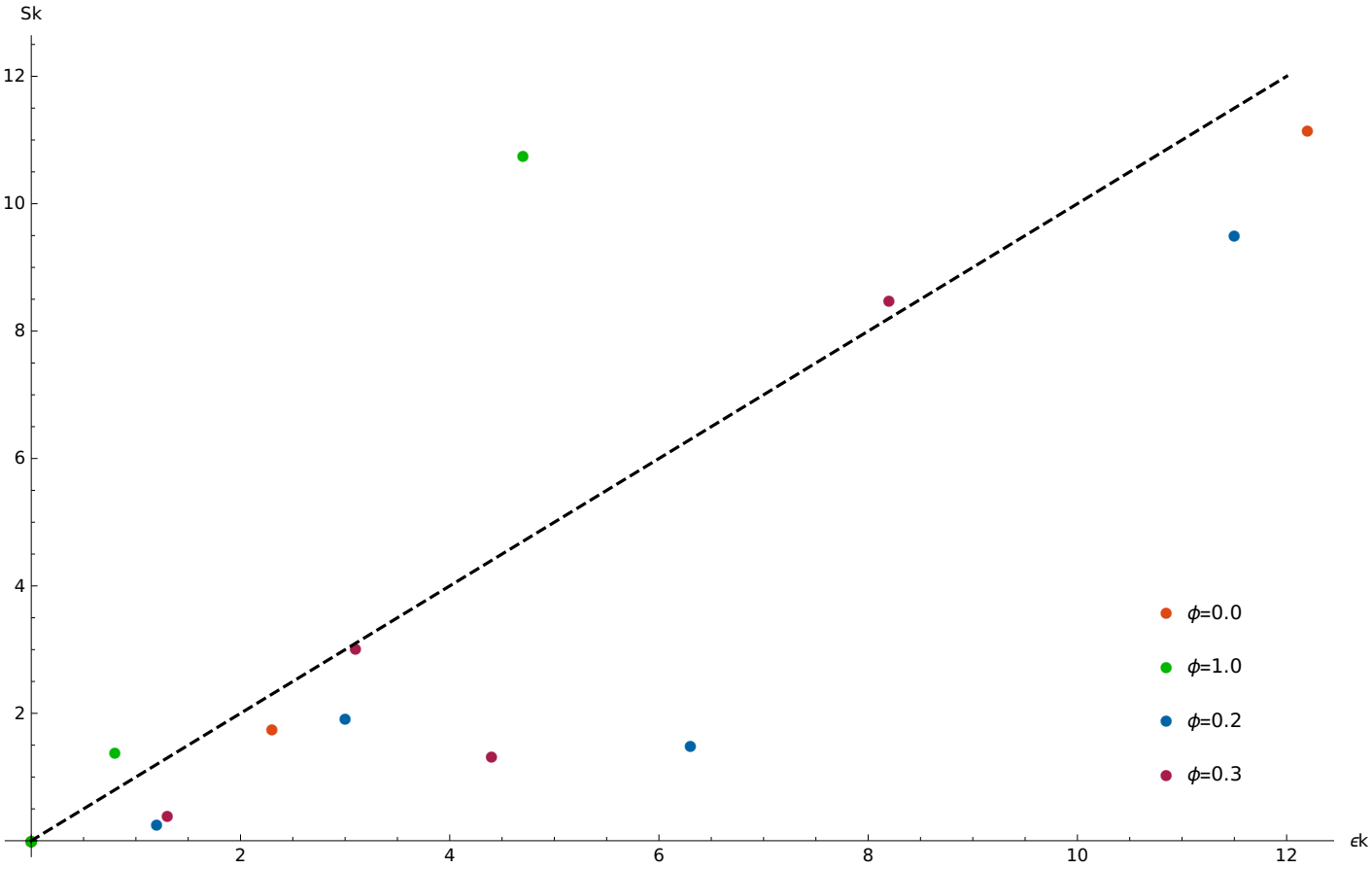

Figure S5: Correlation of the Cavell amplitudes S_k and the partial permittivities $\epsilon_k(0)$ as a function of the composition ϕ_{IL} of the mixture. In case of $\phi_{IL} = 0.0$ and $\phi_{IL} = 1.0$ only the neutral or charged species contribute.

line corresponds to the agreement between S_k and $\epsilon_k(0)$. As visible, there are many outliers to this correlation. Please keep in mind that $\epsilon_k(0)$ is not directly accessible by the experiment as the dielectric conductivity $\vartheta_0(0)$ contribution may overlap with the permittivity. Furthermore, even permittivity contributions of several molecular species overlap resulting in a sum amplitude.

The mutual alignment of dipoles can be characterized by the Kirkwood g_k-factor. However, as the outliers are above and below the optimal line, extremely strong parallel and antiparallel alignments have to be present in these cases. This seems very unrealistic.

2.5 The Voronoi shell-resolved PMF

Based on Voronoi tesselation, the coordination number N_{kl} and the shell-resolved potential of mean force $PMF(s)$ can be computed. In Table S11 the central ion k correspond to the rows of the table. The columns concern the neighboring species l. Although the coordination numbers are symmetric, *i.e.* $N_{kl} = N_{lk}$, the corresponding $PMF_{kl} \neq PMF_{lk}$ are not as the volume of the first shell $V_k(s = 1) \neq V_l(s = 1)$ around the species k and l differ for $l \neq k$.

Table S11: Coordination numbers (N_{kl}) and Potential of mean force (PMF) for λ=0.25.

ϕ_{IL}		N_{kl}				PMF [kJ/mol]			
		Im_1H^+	OAc^-	Im_1	HOAc	Im_1H^+	OAc^-	Im_1	HOAc
0.0	Im_1H^+	-	-	-	-	-	-	-	-
	OAc^-	-	-	-	-	-	-	-	-
	Im_1	-	-	8.40	7.95	-	-	-0.05	0.09
	HOAc	-	-	7.95	5.89	-	-	-0.28	0.47
0.1	Im_1H^+	1.09	1.85	6.75	6.60	-0.76	-2.1	0.15	0.20
	OAc^-	1.85	0.35	5.88	5.18	-2.52	1.75	0.08	0.40
	Im_1	0.75	0.65	7.74	7.22	0.25	0.60	-0.09	0.08
	HOAc	0.73	0.58	7.22	5.31	-0.07	0.54	-0.29	0.47
0.2	Im_1H^+	2.05	2.64	5.94	5.74	-0.61	-1.25	0.19	0.28
	OAc^-	2.64	0.77	5.27	4.57	-1.66	1.45	0.08	0.43
	Im_1	1.49	1.32	7.07	6.51	0.29	0.59	-0.15	0.06
	HOAc	1.44	1.14	6.51	4.77	-0.01	0.56	-0.32	0.45
0.3	Im_1H^+	2.87	3.32	5.25	5.01	-0.42	-0.78	0.19	0.31
	OAc^-	3.32	1.21	4.71	4.01	-1.20	1.32	0.04	0.45
	Im_1	2.25	2.02	6.35	5.79	0.28	0.55	-0.20	0.03
	HOAc	2.15	1.72	5.79	4.22	0.01	0.56	-0.36	0.43
0.4	Im_1H^+	3.69	3.94	4.56	4.32	-0.30	-0.47	0.18	0.32
	OAc^-	3.94	1.67	4.16	3.48	-0.90	1.25	-0.02	0.43
	Im_1	3.04	2.77	5.58	5.04	0.25	0.48	-0.25	-0.003
	HOAc	2.88	2.32	5.04	3.64	-0.01	0.53	-0.39	0.42
0.5	Im_1H^+	4.53	4.63	3.83	3.57	-0.24	-0.29	0.18	0.36
	OAc^-	4.63	2.20	3.55	2.91	-0.72	1.13	-0.06	0.44
	Im_1	3.83	3.55	4.77	4.30	0.23	0.42	-0.31	-0.06
	HOAc	3.57	2.91	4.30	3.13	0.02	0.53	-0.45	0.35
0.7	Im_1H^+	6.16	5.94	2.41	2.19	-0.12	-0.03	0.10	0.35
	OAc^-	5.94	3.33	2.29	1.79	-0.48	0.96	-0.22	0.40
	Im_1	5.63	5.35	2.84	2.69	0.11	0.23	-0.30	-0.16
	HOAc	5.10	4.17	2.69	1.97	-0.03	0.47	-0.55	0.23
0.9	Im_1H^+	7.87	7.34	0.85	0.77	-0.08	0.10	-0.001	0.25
	OAc^-	7.34	4.64	0.81	0.65	-0.37	0.78	-0.34	0.21
	Im_1	7.64	7.26	1.00	0.83	0.002	0.13	-0.35	0.10
	HOAc	6.90	5.82	0.83	0.50	-0.16	0.27	-0.31	0.96
1.0	Im_1H^+	8.80	8.13	-	-	-0.07	0.12	-	-
	OAc^-	8.13	5.35	-	-	-0.36	0.69	-	-
	Im_1	-	-	-	-	-	-	-	-
	HOAc	-	-	-	-	-	-	-	-

2.6 Hydrogen bond lifetimes

Hydrogen bond lifetimes were analysed between the hydrogen atoms of Im_1H^+ and HOAc to the oxygen atoms of HOAc or OAc^- and the nitrogen atom of Im_1[4]. A biexponential fit

$$C(t) = A \cdot \exp\left(\frac{-t}{\tau_1}\right) + B \cdot \exp\left(\frac{-t}{\tau_2}\right) \tag{11}$$

was used to extract the average life time as $A \cdot \tau_1 + B \cdot \tau_2$ given in Table S12. Since these life times are quite short, we do not expect an overstabilization of them due to the induced dipoles.

Interestingly, the hydrogen bonds to N2 of the neutral 1-methylimidazole have the longest life time. Also, the hydrogen bonds between acetic acid dimers have a very short life time in our polarizable simulations.

Table S12: Hydrogen Bond lifetimes

	life time [ps]		
Species	O_{HOAc}	O_{OAc^-}	N_{Im_1}
H_{HOAc}	0.62	1.87	2.75
$H_{Im_1H^+}$	0.43	1.63	2.63

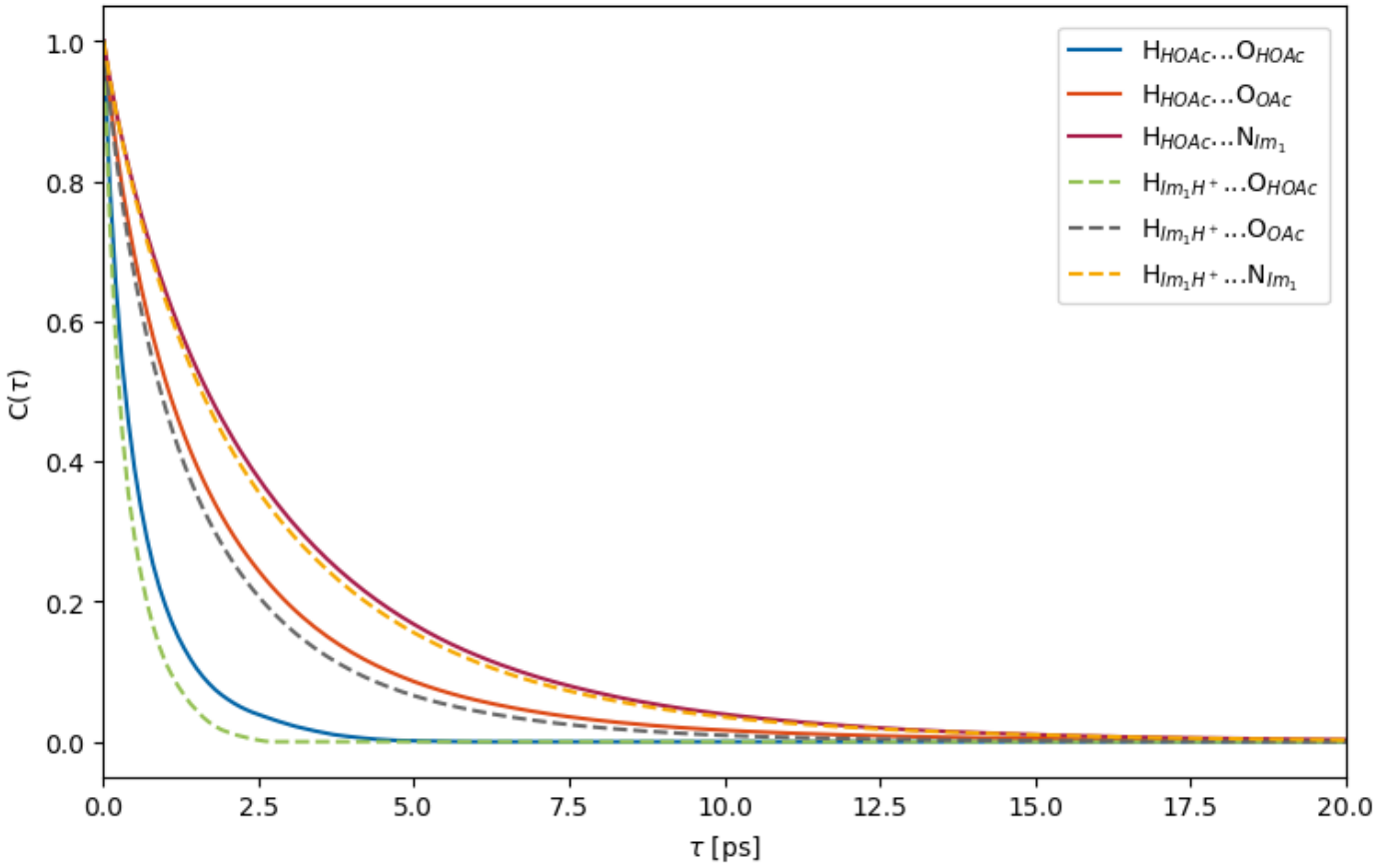

Figure S6: Hydrogen bond lifetimes of the different species.

References

[1] E. Rilo, J. Vila, S. García-Garabal, L. M. Varela and O. Cabeza, *J. Phys. Chem. B*, 2013, **117**, 1411–1418.

[2] C. E. S. Bernardes, K. Shimizu, J. N. C. Lopes, P. Marquetand, E. Heid, O. Steinhauser and C. Schröder, *Phys. Chem. Chem. Phys.*, 2016, **18**, 1665–1670.

[3] E. A. S. Cavell, P. C. Knight and M. A. Sheikh, *Trans. Faraday Soc.*, 1971, **67**, 2225–2233.

[4] P. Smith, R. M. Ziolek, E. Gazzarrini, D. M. Owen and C. D. Lorenz, *Phys. Chem. Chem. Phys.*, 2019, **21**, 9845–9857.